Hum Genet (2015) 134:553–568
DOI 10.1007/s00439-015-1535-8

ORIGINAL INVESTIGATION

Exome sequencing unravels unexpected differential diagnoses in individuals with the tentative diagnosis of Coffin–Siris and Nicolaides–Baraitser syndromes

Nuria C. Bramswig · Hermann-Josef Lüdecke · Yasemin Alanay · Beate Albrecht · Alexander Barthelmie · Koray Boduroglu · Diana Braunholz · Almuth Caliebe · Krystyna H. Chrzanowska · Johanna Christina Czeschik · Sabine Endele · Elisabeth Graf · Encarna Guillén-Navarro · Pelin Özlem Simsek Kiper · Vanesa López-González · Ilaria Parenti · Jelena Pozojevic · Gulen Eda Utine · Thomas Wieland · Frank J. Kaiser · Bernd Wollnik · Tim M. Strom · Dagmar Wieczorek

Received: 2 December 2014 / Accepted: 9 February 2015 / Published online: 28 February 2015

Abstract Coffin–Siris syndrome (CSS) and Nicolaides–Baraitser syndrome (NCBRS) are rare intellectual disability/congenital malformation syndromes that represent distinct entities but show considerable clinical overlap. They are caused by mutations in genes encoding members of the BRG1- and BRM-associated factor (BAF) complex. However, there are a number of patients with the clinical diagnosis of CSS or NCBRS in whom the causative mutation has not been identified. In this study, we performed trio-based whole-exome sequencing (WES) in ten previously described but unsolved individuals with the tentative diagnosis of CSS or NCBRS and found causative mutations in nine out of ten individuals. Interestingly, our WES analysis disclosed overlapping differential diagnoses including Wiedemann–Steiner, Kabuki, and Adams–Oliver syndromes. In addition, most likely causative de novo mutations were identified in *GRIN2A* and *SHANK3*. Moreover, trio-based WES detected *SMARCA2* and *SMARCA4* deletions, which had not been annotated in a previous Haloplex target enrichment and next-generation sequencing of known CSS/NCBRS genes emphasizing the advantages of WES as a diagnostic tool. In summary, we discuss the phenotypic and diagnostic challenges in clinical genetics, establish important differential diagnoses, and emphasize the cardinal features and the broad clinical spectrum of BAF complex disorders and other disorders caused by mutations in epigenetic landscapers.

Electronic supplementary material The online version of this article (doi:10.1007/s00439-015-1535-8) contains supplementary material, which is available to authorized users.

N. C. Bramswig (✉) · H.-J. Lüdecke · B. Albrecht · A. Barthelmie · J. C. Czeschik · D. Wieczorek
Institut für Humangenetik, Universitätsklinikum Essen, Universität Duisburg-Essen, Hufelandstr. 55, 45122 Essen, Germany
e-mail: nuria.braemswig@uni-due.de

Y. Alanay
Department of Pediatrics, School of Medicine, Acibadem University, Istanbul, Turkey

Y. Alanay · K. Boduroglu · P. Ö. S. Kiper · G. E. Utine
Department of Pediatric Genetics, Ihsan Dogramaci Children's Hospital, Hacettepe University School of Medicine, Ankara, Turkey

A. Barthelmie
Institut für Radiologie, Kantonsspital Baden AG, Baden, Switzerland

D. Braunholz · I. Parenti · J. Pozojevic · F. J. Kaiser
Sektion für Funktionelle Genetik am Institut für Humangenetik, Universität zu Lübeck, Lübeck, Germany

A. Caliebe
Institut für Humangenetik, Christian-Albrechts-Universität zu Kiel, Kiel, Germany

K. H. Chrzanowska
Department of Medical Genetics, The Children's Memorial Health Institute, Warsaw, Poland

S. Endele
Institut für Humangenetik, Friedrich-Alexander-Universität Erlangen-Nürnberg, Erlangen, Germany

E. Graf · T. Wieland · T. M. Strom
Institute of Human Genetics, Helmholtz Zentrum München, Neuherberg, Germany

E. Guillén-Navarro · V. López-González
Sección de Genética Médica, Servicio de Pediatría, Hospital Clínico Universitario Virgen de la Arrixaca, IMIB-Arrixaca, Murcia, Spain

E. Guillén-Navarro · V. López-González
CIBERER-ISCIII Madrid, Madrid, Spain

Introduction

Coffin–Siris syndrome (CSS) (OMIM #135900) was first described by Coffin and Siris (1970). It is a rare congenital syndrome, which is characterized by a combination of developmental delay and/or intellectual disability (ID), hypo/aplasia of the fifth digit or finger-/toenail, coarseness of the face with thick eyebrows, a broad nasal bridge and nasal tip, a wide mouth and thick vermillion of the upper and lower lip. In addition, affected individuals may present with short stature and microcephaly, hirsutism and sparse scalp hair (Kosho and Okamoto 2014). In 2012, mutations in genes encoding for members of the SWItch/Sucrose NonFermentable (SWI/SNF) complex were identified as the cause for CSS and included the genes *ARID1A*, *ARID1B*, *SMARCA4*, *SMARCB1* and *SMARCE1* (Santen et al. 2012; Tsurusaki et al. 2012). Recently, two missense mutations in *SOX11*, a transcription factor downstream of the PAX6-BAF complex, were described in two patients with CSS (Tsurusaki et al. 2014). The SWI/SNF complex mobilizes nucleosomes and remodels chromatin in an ATP-dependent manner (Wilson and Roberts 2011). It facilitates access of transcription factors to regulatory regions of target genes and thereby regulates gene expression. Interestingly, mutations in *SMARCA2*, a gene encoding for another subunit of the SWI/SNF complex, have been shown to be causative for Nicolaides–Baraitser syndrome (NCBRS) (OMIM #601358) (Van Houdt et al. 2012). NCBRS was first described by Nicolaides and Baraitser (1993) and well delineated in 2009 (Sousa et al. 2009). Clinical characteristics include severe ID, seizures, sparse scalp hair, progressive facial coarsening with thick nares, broad philtrum, wide mouth and thin upper and thick lower vermillion. In addition, individuals with NCBRS can show microcephaly, short stature, short metacarpals and/or metatarsals, prominent interphalangeal joints and broad distal phalanges. The SWI/SNF complex has also been termed the BRG1- and BRM-associated factor (BAF) complex, which in turn has led to term "BAFopathy" describing SWI/SNF complex-related disorders.

Apart from the remarkable clinical overlap between CSS and NCBRS, mutations in other chromatin remodeling complexes or associating factors have been observed in similar phenotypes. For example, mutations in *PHF6*, originally known as the causative gene for Borjeson–Forssman–Lehmann syndrome (OMIM #301900) (Berland et al. 2011; Crawford et al. 2006; Lower et al. 2002), can also lead to a CSS-like phenotype in females at a young age (Wieczorek et al. 2013; Zweier et al. 2014). The PHF6 protein interacts with the nucleosome remodeling and deacetylation (NuRD) complex, but does not have a known association with the BAF complex. This observation suggests that similar pathophysiological mechanisms, i.e., nucleosome remodeling, may lead to clinically overlapping phenotypes. Taken together, these findings emphasize the complexity of proper maintenance of the epigenetic landscape, point at interactions between histone and nucleosome landscape modifiers and suggest potential clinical overlap between entities caused by mutations in epigenetic modifiers.

In this study, we performed trio-based whole-exome sequencing (WES) in ten previously unsolved individuals with an initial clinical diagnosis of CSS/NCBRS from the patient cohort described by Wieczorek et al. (2013). The aim of this study was the analysis of individuals resembling the phenotypes of the CSS/NCBRS spectrum by WES, to detect novel variants, disease genes and differential diagnoses and to assess the variability of CSS/NCBRS. Using this approach, we reveal important differential diagnoses and emphasize the wide clinical spectrum of CSS and NCBRS. Strikingly, differential diagnoses included the Wiedemann–Steiner (OMIM #605130) and Kabuki syndromes (OMIM #147920), which are caused by mutations in genes encoding for two histone methyltransferases. These results indicate that mutations in different factors shaping the epigenetic landscape lead to a broad clinical spectrum with considerable clinical overlap.

Materials and methods

Subjects

Individuals with the initial diagnosis of CSS or NCBRS and their parents were clinically assessed and diagnosed by the respective clinical geneticists. The individuals were

E. Guillén-Navarro
Cátedra de Genética, UCAM-Universidad Católica de Murcia, Murcia, Spain

I. Parenti
Department of Health Sciences, Medical Genetics, Università degli Studi di Milano, Milan, Italy

B. Wollnik
Institute of Human Genetics, University of Cologne, Cologne, Germany

B. Wollnik
Center for Molecular Medicine Cologne (CMMC), University of Cologne, Cologne, Germany

B. Wollnik
Cologne Excellence Cluster on Cellular Stress Responses in Aging-Associated Diseases (CECAD), University of Cologne, Cologne, Germany

T. M. Strom
Institute of Human Genetics, Technische Universität München, Munich, Germany

initially published in a study from Wieczorek et al. (2013). This study included 46 individuals with an initial diagnosis of CSS/NCBRS, of which 28 individuals were solved in the course of the previous study. Of the remaining 18 patients, we selected ten patients of whom parental DNA was available using the following criteria: ID/developmental delay in individuals older than 6 months combined with at least one of the following features: fifth nail hypoplasia, coarse face, sparse hair. Clinical information was provided by the parents or legal guardians for minors and by the evaluating authors. Written informed consent was obtained from the families of the index individuals for participation in this study. The study was performed according to the Declaration of Helsinki protocols and was approved by the local institutional review board (ethical votum 12-5089-BO for CRANIRARE, 08-3663 for MRNET and 5360/13 for the Technical University Munich). Blood samples were collected from the affected individuals and their parents and DNA was extracted from peripheral blood lymphocytes by standard extraction procedures.

Molecular karyotyping

Array comparative genomic hybridization (array-CGH) was performed using the following array types and analysis tools. The Affymetrix 6.0 SNP array was used in the individuals K2430, K2431, K2468 and K2512; the CytoScanHD array was utilized in the individuals K2446, K2589 and K2576 (Affymetrix, Santa Clara, CA, USA); the 180k-array (Agilent, Santa Clara, CA, USA) was used in the individual K2571; the 44k-array (Agilent, Santa Clara, CA, USA) was used in the individual K2690; the BAC array (Cytochip v3.01, BlueGnome, Cambridge, UK) was used in individual K2510 according to the manufacturer's instructions. Data analysis was carried out using the Affymetrix Chromosome Analysis Suite (ChAS v1.2 or v2.0), Genotyping Console (GTC v4.1), Software Agilent Genomic Workbench v6.5 or BlueFuse v3.6 (BlueGnome, Cambridge, UK) and the data interpretation was based on the February 2009 human genome sequence assembly (GRCh37/hg19). Conspicuous regions were compared with known CNVs, as provided by the Database of Genomic Variants (http://projects.tcag.ca/variation/).

Haloplex target enrichment followed by next-generation sequencing

In the previous study (Wieczorek et al. 2013), Haloplex target enrichment followed by next-generation sequencing was performed on coding exons and exon–intron boundaries of the following known CSS and candidate genes: *ARID1A* (NM_006015.4), *ARID1B* (NM_020732.3), *SMARCA2* (NM_003070.3), *SMARCA4* (NM_001128849.1), *SMARCB1* (NM_003073.3), *SMARCE1* (NM_003079.4), *ARID2* (NM_152641.2), *SMARCC1* (NM_003074.3), *SMARCC2* (NM_003075.3), *SMARCD1* (NM_003076.4), *SMARCD2* (NM_001098426.1), *SMARCD3* (NM_003078.3), *ACTL6A* (NM_004301.3), *ACTL6B* (NM_016188.4), *PBRM1* (NM_018313.4), *BRD7* (NM_001173984.2), *PRMT5* (NM_006109.3), *SMARCA1* (NM_003069.3), *SMARCA5* (NM_003601.3), *HELLS* (NM_018063.3), *CBL* (NM_005188.3), *C7orf11* (NM_138701), and *SHOC2* (NM_007373.3). This analysis did not detect pathogenic sequence variants, deletions or duplications in the ten presented individuals. This analysis was performed on all individuals presented in this paper.

Exome sequencing

We performed trio-based WES in a cohort of ten patients with the tentative diagnosis of CSS/NCBRS (Wieczorek et al. 2013). Exomes were enriched using the SureSelect XT Human All Exon 50 Mb kit, version 5 (Agilent Technologies). Sequencing was performed on HiSeq 2500 systems (Illumina). Reads were aligned against the human assembly hg19 (GRCh37) using Burrows–Wheeler Aligner (BWA v 0.7.5). We performed variant calling using SAMtools (v 0.1.18), PINDEL (v 0.2.4t) and ExomeDepth (v1.0.0). Subsequently, variants were filtered using the SAMtools varFilter script and custom scripts. The variants were then inserted into an in-house database. To discover putative de novo variants, we queried the database to show only those variants of a child that were not found in the corresponding parents. Pathogenic de novo variants and the compound heterozygous variants in individual K2576 were verified by Sanger sequencing, primer sequences will be provided upon request.

Quantitative real-time PCR and Sanger sequencing

The presence of the *SMARCA4*-intragenic deletion in individual K2430 was confirmed by a quantitative real-time PCR assay using the Roche Universal ProbeLibrary System and by Sanger sequencing of the deletion junction fragment. Two segments of *SMARCA4* [chr19:11,152,435-11,152,503 (intron 31) and chr19:11,169,426-11,169,487 (intron 32/exon 33)] were amplified with primers *SMARCA4*_1: 5′-CGGTGATGAGAGGGAATGTC-3′ and *SMARCA4*_2: 5′-GTCCCCTTCTCCGAGACC-3′ as well as *SMARCA4*_3: 5′-GGTCCTGAGGTAAGACCTGCT-3′ and *SMARCA4*_4: 5′-GTACTTGTGGTTGCGAATGC-3′ and detected with the universal probes 34 or 86, respectively. The analysis was performed on the LightCycler 480 (Roche), and data were analyzed with the 'advanced relative quantification' method which is implemented in the LightCycler 480 software (v1.5).

Assessment of the *SMARCA4* deletion breakpoints

We performed deletion spanning PCR and Sanger sequencing to determine the deletion breakpoints of the *SMARCA4*-intragenic deletion in individual K2430. The deletion junction fragment was amplified from the patient's genomic DNA using the primers *SMARCA4*_intron29: 5′-TGTCCTG AAGCAATAATTCCGAG-3′ and *SMARCA4*_exon36: 5′-CCATCTCAGCTCTGGAACGA-3′. In wild-type genomic DNA, the 3′ ends of the primers are 25,897 bp apart, and thus would not yield a PCR product under standard conditions. However, from the patient's genomic DNA, they amplify a 286-bp product.

Results

Whole-exome sequencing reveals *SMARCA2* and *SMARCA4* variants

We performed WES in ten unsolved individuals with a tentative clinical diagnosis of CSS/NCBRS (Wieczorek et al. 2013) and detected 0–4 de novo variants per individual. In combination with the clinical data, we selected the most likely pathogenic variant, which we are presenting below. The most relevant clinical features are summarized in Table 1, a more extensive overview of the clinical features is provided in supplemental Table 1 (template provided by Prof. Dr. Raoul Hennekam). Despite previous Haloplex enrichment followed by next-generation sequencing of the known CSS/NCBRS genes, WES identified pathogenic *SMARCA2* and *SMARCA4* variants in the following four out of ten individuals.

Individual K2510 is the third child of healthy, non-consanguineous parents of Pakistani origin. He has two first-degree cousins with intellectual disability from a consanguineous marriage of his maternal uncle and a relative. Pregnancy was uneventful until CTG deterioration was noted in week 36, because of which Cesarean section was performed. His birth weight was 1980 g (−1.98 SD), length 45 cm (−1.58 SD) and occipital frontal circumference (OFC) 32.5 cm (−0.81 SD); APGAR index was 10/10 and umbilical artery pH 7.32. Telangiectasia around the nostrils and facial dysmorphisms (micrognathia, macrostomia) were noted after birth. Because of his low birth weight, he was transferred to the pediatric hospital and was monitored for 2 weeks. Hydrocele testis, microcephaly, and low weight were noted at 1 month of age, plagiocephaly and umbilical hernia at 6 months of age. The hernia was corrected surgically at 9 months. He started walking at 18 months of age and had his first epileptic seizures at 18 months as well. EEG repeatedly showed abnormal rhythms. At 2 $^{9}/_{12}$ years, cryptorchidism was corrected surgically. Cranial magnetic resonance imaging (MRI) at age 1 $^{8}/_{12}$ years showed microcephaly, but no other pathological findings. Hand X-ray at age 3 $^{6}/_{12}$ years showed a mildly delayed bone age of 3 $^{1}/_{12}$ years. X-rays of the pelvis showed mild coxa valga. When the patient was presented in the clinic, he was 3 $^{6}/_{12}$ years old, had a height of 98 cm (−0.25 SD), a weight of 13 kg (−1.52 SD, BMI: 13.53 kg/m^2) and an OFC of 47 cm (−2.52 SD). He showed micrognathia, macrostomia, a short philtrum, cupid's bow of the upper lip and a hypertrichosis of forehead, lateral cheeks and ears; scalp hair was sparse. Excess skin on the hands was noted. He had no speech, was not able to eat with a spoon and was not toilet-trained. His mother reported excessive sleepiness during the day since the initiation of a new combination therapy with anticonvulsive substances (oxcarbazepine and levetiracetam) for his previously intractable epilepsy. At a follow-up examination at age 6 $^{8}/_{12}$ years (Fig. 1a–d), the patient had a height of 122 cm (−0.32 SD), a weight of 28 kg (+1.37 SD, BMI: 18.81 kg/m^2) and an OFC of 51 cm (−0.73 SD). He still had no speech and received special education. Seizure frequency was reduced to four to five seizures in the last 10 months under a medication with lacosamide and levetiracetam plus ketogenic diet. The clinical diagnosis was NCBRS. WES revealed a de novo, heterozygous missense mutation in the *SMARCA2* gene [chr9:g.2,086,944G>A; c.2642G>A; p.(Gly881Glu)]. This *SMARCA2* variant was rated as probably pathogenic in PolyPhen-2 (http://genetics.bwh.harvard.edu/pph2/) and the clinical diagnosis of NCBRS was confirmed.

This individual (K2589) is the first child of healthy, non-consanguineous parents. The mother had a previous miscarriage, otherwise the family history was uneventful. The patient was born at 42 weeks of gestation with a weight of 3820 g (+0.51 SD), a length of 58 cm (+0.51 SD) and OFC of 36 cm (−0.1 SD). He was diagnosed with a patent foramen ovale (PFO), central hypotonia, peripheral hypertonia, bilateral inguinal hernia and cryptorchidism. He underwent three surgeries: first at the age of 1 month for the right inguinal hernia, then at the age of 1 year for the left inguinal hernia and left orchidopexy, and at the age of 1.5 years for right orchidopexy and recurrence of the right inguinal hernia. He sat at the age of 8 months, walked independently at 14 months and said his first words at about 36 months. MRI of the brain and metabolic diagnostics, as well as sleep EEG were normal. Abdominal ultrasonography did not show any abnormality. His first assessment was at the age of 1 $^{4}/_{12}$ years (Fig. 1e–g) when his height was 80.2 cm (−0.54 SD), his weight was 9.1 kg (−1.96 SD, BMI: 14.15 kg/m^2), and his OFC was 47.5 cm (−0.62 SD). Facial dysmorphisms included triangular shape of face with malar flattening, downslanted palpebral fissures, hypertelorism, a broad nasal root, long and flat philtrum,

Table 1 Clinical data of cohort with a tentative diagnosis of CSS and NCBRS

	K2510	K2589	K2690	K2430	K2431	K2571	K2576	K2468	K2512	K2446
Gene with pathogenic variant	*SMARCA2* c.2642G>A; p.(Gly881Glu)	*SMARCA2* c.3655G>C; p.(Ala1219Pro)	*SMARCA2* c.3457_3462delGATCTG; p.(Asp1153_Leu1154del)	*SMARCA4* chr 19:g.11,146,701_11,172,353del	*KMT2A* c.3464G>A; p.(Cys1155Tyr)	*KMT2D* c.5943delC; p.(Ser1928Pro*fs**65)	*DOCK6* c.3437A>G; p.(His1146Arg) paternal. c.5362-1G > T maternal	*GRIN2A* c.4189_4193delAATGA; p.(Asn1397Gln*fs**23)	*SHANK3* c.2265 + 1G>A	–
Age at diagnosis [mo]	54	40	114	20	22	<1	11	88	188	17
Gender	Male	Male	Female	Female	Male	Male	Female	Male	Male	Female
Consanguinity in parents	–	Not recorded (n.r.)	–	–	–	–	–	–	–	–
Age of mother at birth [years]	35	32	25	21	24	37	24	26	24	28
Age of father at birth [years]	35	31	29	31	31	41	25	28	26	36
ID	++	++	+	+	+	/	+	++	++	+
Sat/walked independently [mo]	n.r./18	8/14	n.r./16	9/18	>12/–	/	12/18	18/24	8/14	42/–
First words [mo]	–	36	24	18	–	/	15	33	No speech; echolalia	15
Hypotonia	+	+	–	+	+	/	–	n.r.	–	+
Seizures [years]	+ [1 6/12]	–	+ [0 9/12]	–	–	/	–	+[9 3/12]	+ [12]	–
Vision problem	n.r.	–	–	–	+, Right retinal atrophy	/	Retinopathy of prematurity	n.r.	Strabismus convergens, hypermetropia	–
Hearing loss	(+)	–	–	–	–	/	n.r.	n.r.	–	–
Frequent infections	–	+	–	–	+	/	–	–	+	–
Feeding problems	–	+	+ (Cow´s milk protein intolerance)	–	+	/	+	+	+	+
Behavioral anomalies	–	Hyperactivity, tantrums	+ (Hyperactivity)	Autism	–	/	–	Autism, restless	Autism, sleeplessness	–
Birth [weeks]	36	42	40	40	40	38	32	38	40	40
Weight [g]/[SD]	1980/−1.98	3820/0.51	3200/0.04	3120/−0.8	2150/−3.3	2870/−1.2	1110/−1.74	3270/−0.1	3810/0.42	3500/0.06
Length [cm]/[SD]	45/−1.58	58/0.51	51/0.94	n.r.	n.r.	50/0.1	37/−1.7	54/1.6	55/1.1	n.r.
OFC [cm]/[SD]	32.5/−0.81	36/−0.1	34.5/0.17	n.r.	n.r.	32/−1.8	27/−1.47	35/0.07	36/0.3	n.r.
Age at examination [years]	6 8/12	4 4/12	11 8/12	1 8/12	1 10/12	4 days	1 8/12	7 4/12	13 11/12	4
Height [cm]/[SD]	122/−0.32	101.4/−1.38	140/−1.59	84/1.3	71/−4.46	/	74/−2.94	131/1.23	147/−1.93	93/−1.9
OFC [cm]/[SD]	51/−0.73	51/−0.5	52/−1.6	46/−1.1	42/−4.6	/	44.5/−2.64	54/1.43	52/−1.71	43/-4.95
Craniofacial anomalies										
Coarse face	+	+	+	+	+	+	+	+	+	+
Low frontal hairline	+	+	–	+	+	–	–	–	+	+
Synophrys	–	–	–	–	–	–	–	–	+	+
Thick eyebrows	+	+	+	+	+	–	–	+	+	+
Long eyelashes	+	+	+	+	+	–	+	+	+	+

Table 1 continued

	K2510	K2589	K2690	K2430	K2431	K2571	K2576	K2468	K2512	K2446
Ptosis	+	−	+	+	−	−	−	+	−	+
Narrow palpebral fissures	−	−	−	−	−	−	+	−	−	−
Flat nasal bridge	+	−	+	+	+	+	+	+	−	+
Broad nose	+	+	+	+	+	+	+	−	−	+
Upturned nasal tip	−	+	+	+	+	+	+	−	−	−
Thick, anteverted alae nasi	+	+	+	−	−	+	+	−	−	+
Large mouth	+	+	+	+	+	+	−	+	+	+
Thin upper vermillion	−	+	+	+	+	+	+	+	−	−
Thick lower vermillion	+	+	+	+	+	+	−	+	+	+
Macroglossia	−	−	−	−	+	−	−.	−	+	+
Short philtrum	+	−	−	−	−	−	−	−	+	+
Long philtrum	−	+	+	+	+	+	+	+	−	−
Abnormal ears	−	Protruding, posteriorly rotated	+	Small, protruding	−	+	−	Small, protruding	−	+
Cleft palate	−	−	−	−	−	−	Highly arched palate	n.r.	−	−
Skeletal anomalies										
A/Hypoplasia of distal phalanges V	−	Mild	+	+	+	Generally short distal phalanges	Generally short distal phalanges; very short toes on left foot	Generally short distal phalanges	Generally short distal phalanges	+
Short metacarpals/metatarsals	−	n.r.	+	n.r.	n.r.	n.r.	n.r.	n.r.	n.r.	n.r.
Prominent interphalangeal joints	+	Mild	+	+	+	−	−	−	−	+
Prominent distal phalanges	+	Mild	+	−	+	−	−	−	−	+
Sandal gap	+	+	+	−	−	−	−	−	−	−
Spinal anomalies	n.r.	−	n.r.	−	−	Cervical rib C7, butterfly vertebra Th10	n.r.	n.r.	n.r.	−
Delayed bone age	−	+	n.r.	n.r.	n.r.	n.r.	n.r.	n.r.	n.r.	n.r.
Scoliosis	−	−	−	−	−	−	n.r.	−	−	−
Internal anomalies										
Cryptorchidism	+	+		/	+	n.r.	/	−	n.r.	−
CHD	−	PFO	Non-compaction cardiomyopathy	−	PDA, MVP	Hypoplastic left heart	PFO, VSD	ASD, VSD, aortic insufficiency	−	−
Ectodermal anomalies										
Body hirsutism	+	−	+	−	+	−	−	−	+	+
Increased skin wrinkling	+	+	+	−	−	−	+	−	−	+
Fetal finger pads	+	−	−	+	−	First toe	−	−	n.r.	−

Table 1 continued

	K2510	K2589	K2690	K2430	K2431	K2571	K2576	K2468	K2512	K2446
Sparse scalp hair	+	+	+	+	+	/	Localized hair thinning	−	−	+
Nail a/hypoplasia	−	+	−	+	−	+	+	−	−	+
Hands V	−	All fingernails	−	+	+	+	+	−	−	+
Feet V	−	−	−	bil	−	+	++ (left > right)	−	+	−
Delayed dentition	n.r.	−	−	n.r.	n.r.	/	n.r.	−	n.r.	−
Brain anomalies										
Small cerebellum	−	n.r.	−	−	−	−	−	−	−	−
Dandy–Walker anomaly	−	n.r.	−	−	−	−	−	−	−	−
Abnormal corpus callosum	−	n.r.	−	+	no	−	−	−	−	−
Others	Umbilical and inguinal hernia	Umbilical and inguinal hernia, hypothyroidism	Umbilical and inguinal hernia	−	Fasciculation of tongue	Diaphragmatic hernia, agenesis of left kidney, corneal clouding, pectus excavatum	Umbilical and inguinal hernia	−	Hoarse voice	−

PFO patent foramen ovale, *PDA* patent ductus arteriosus, *MVP* mitral valve prolapse, *VSD* ventricular septal defect, *ASD* atrial septal defect

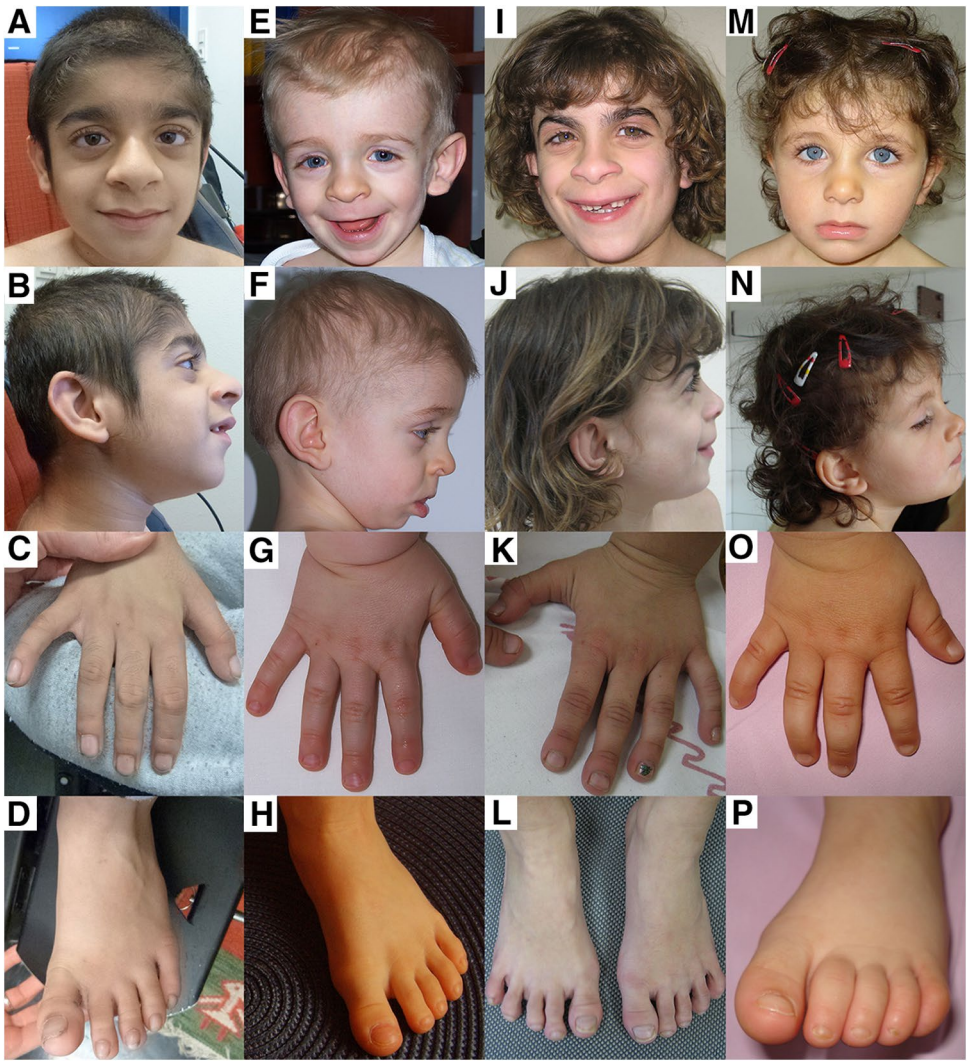

Fig. 1 Clinical photographs of patients with mutations or deletions in members of the BAF complex. **a–d** K2510 at the age of 6 $^{8}/_{12}$ years (*SMARCA2* missense mutation). Please note that this patient presents with sparse hair, but full lower lip and thickened interphalangeal joints are not present. He displays an unusual phenotype for NCBRS. **e–h** K2589 (*SMARCA2* missense mutation). This patient presents with the typical facial dysmorphisms for NCBRS. Most likely due to his young age (1 $^{4}/_{12}$ years) he does not have prominent interphalangeal joints. He has hypoplastic fingernails. The picture in 1H was taken at the age of 5 $^{4}/_{12}$ years. **i–l** K2690 (intragenic *SMARCA2* deletion) at the age of 11 $^{8}/_{12}$ years, she has the typical facial phenotype for NCBRS. **m–p** K2430 (intragenic *SMARCA4* deletion) presents with mild facial dysmorphism at the age of 1 $^{8}/_{12}$ years, but hypoplastic nails, especially fifth toe and fingernail leading to the diagnosis CSS

a full lower vermillion, as well as protruding ears (Fig. 1e, f). His hair was sparse. His last auxologic assessment at the age of 4 $^{4}/_{12}$ years revealed: height 101.4 cm (−1.38 SD), weight 15 kg (−1.35 SD, BMI: 14.59 kg/m^2) and OFC 51 cm (−0.5 SD). He presented with mild developmental retardation on psychological assessment at age 4 $^{9}/_{12}$ years using the Brunet–Lezine scale (Malak et al. 2013); his developmental age was calculated as 3 $^{3}/_{12}$ years and his IQ was 68. The age of adaptive behaviors (AB) was assessed as 5 $^{2}/_{12}$ years at the age of 5 $^{4}/_{12}$ with the Vineland Adaptive Behavior Scale (Raggio et al. 1994), and his adaptive behavior quotient (ABQ) was 97, indicating progress of developmental rate. He spoke many single words and was extremely hyperactive. The parents reported that he was never able to eat slowly. Facial dysmorphisms included hypertelorism with long palpebral fissures and long eyelashes, midface hypoplasia and a full lower and thin upper vermillion. His face appeared coarser than in the previous assessment, and hair was sparse and stiff. His hands were short and broad with brachytelephalangy and short fingernails and he had broad feet with no hypoplasia of the toenails (Fig. 1h). The clinical diagnosis was NCBRS. WES revealed a heterozygous, de novo variant in the gene *SMARCA2* [chr9:g.2,116,020G>C; c.3655G>C; p.(Ala1219Pro)]. The *SMARCA2* mutation was rated as probably damaging by PolyPhen-2 confirming the diagnosis of NCBRS.

Individual K2690 is a 12-year-old girl, second child of healthy and non-consanguineous Spanish parents. Her brother aged eight was diagnosed with pervasive developmental disorder–autism spectrum disorder, and there are no other remarkable family data. The girl was born at term by vaginal delivery, after an uneventful pregnancy, with a weight of 3200 g (+0.04 SD), a length of 51 cm (+0.94 SD) and an OFC of 34.5 cm (+0.17 SD). Dysmorphic craniofacial features were evident at birth. Neonatal auditory and metabolic screenings were normal. At 9 months of age, she began to suffer from seizures triggered by fever

and underwent treatment with phenobarbital for a year. EEG and brain MRI showed no abnormalities. She failed to thrive within the first several months of life and was diagnosed with cow's milk protein intolerance, with subsequent proper recovery. At the age of 4 years, she had surgery for umbilical hernia and adenoidal hypertrophy. She showed mild developmental delay with social smile at 3 months, walking at 16 months and first words at 2 years. She attended an early intervention program and a regular school with curriculum accommodation and speech therapy. She showed a restless behavior with attention deficit. She had neither regression nor aggressiveness or sleep disturbances. Her physical exam at the age of 11 $^{8}/_{12}$ years revealed a height of 140 cm (−1.59 SD), a weight of 43 kg (−0.12 SD, BMI: 21.94 kg/m^2) and an OFC of 52 cm (−1.6 SD). She showed sparse hair, coarse facial features, short forehead, thick eyebrows, downslanting palpebral fissures, long eyelashes, infraorbital creases, long philtrum, thick alae nasi, wide nasal base, large mouth, thin vermillion of the upper and thick vermillion of the lower lip, high palate and low-set ears (Fig. 1i, j). The proximal interphalangeal joints were thick with wrinkling skin and distal phalanges of fingers and toes were broad (Fig. 1k, l). Her skin was dry with generalized hirsutism. She presented with mild to moderate intellectual disability. Abdominal ultrasound detected bilateral hydronephrosis that resolved spontaneously. Ophthalmological assessment did not detect anomalies. Cardiac evaluation showed slightly hypertrophied apical trabeculae in both ventricles without fulfilling cardiomyopathy criteria. She had the clinical diagnosis of NCBRS. WES revealed a heterozygous de novo 6-bp deletion within the *SMARCA2* gene [chr9:g.2,115,822-2,115,827; c.3457_3462delGATCTG; p.(Asp1153_Leu1154del)]. The intragenic *SMARCA2* deletion was rated as deleterious by the PROVEAN tool (http://provean.jcvi.org/index.php) supporting the diagnosis NCBRS.

This girl (K2430) is the only child of healthy, non-consanguineous parents with an uneventful family history. The prenatal history was unremarkable. She was born at 40 weeks of gestation with a birth weight of 3120 g (−0.8SD). Her birth length and head circumference were not noted. She was diagnosed with autism at the age of 20 months. She had head control at the age of 6 months, sat without support at 9 months, walked after 18 months and said first words at about 2 years of age. MRI of the brain revealed hypoplasia of corpus callosum. Metabolic diagnostics, the sleep EEG, EMG and echocardiography were normal. She did not have any seizures. Her assessment was at the age of 1 $^{8}/_{12}$ years when her height was 84 cm (+1.3 SD), her weight was 11,500 g (+0.03 SD, BMI: 16.2 kg/m^2) and her OFC was 46 cm (−1.1 SD). She could speak two words. Facial dysmorphisms included coarse face, a broad nasal root, bulbous nasal tip, a full lower vermillion as well as small and protruding ears, long eyelashes, downslanted palpebral fissures and sparse hair (Fig. 1m, n). Especially her fifth finger- and toenails were hypoplastic bilaterally (Fig. 1o, p). She did not have feeding problems, recurrent infections or hearing loss. She had the initial diagnosis of CSS. WES revealed an approximately 26 kb *SMARCA4* intragenic deletion of exons 30 through 35, which was verified by quantitative Real-Time PCR to have occurred de novo. Analysis of the deletion junction fragment by Sanger sequencing of a PCR product generated from the patient's genomic DNA with primers in intron 29 and exon 36 revealed a deletion of 25,652 bp (chr19:g.11,146,701_11,172,353del). The deletion of exons 30 through 35 possibly results in an in-frame deletion of codons 1391 through 1669 and a protein missing 279 internal amino acids. This result established the diagnosis of CSS in the individual K2430.

WES disclosed interesting differential diagnoses to CSS/NCBRS

In five of the remaining six individuals, WES detected pathogenic variants in other interesting disease-associated genes, which are not members of the BAF complex and are described in the following case reports.

Individual K2431 is the second child of healthy, non-consanguineous parents with an uneventful family history. The prenatal history was unremarkable. The boy was born at 40 weeks of gestation with a birth weight of 2150 g (−3.3 SD). The birth length and head circumference were not noted. He received phototherapy for indirect hyperbilirubinemia when he was 23 days old and he had aspiration pneumonia at the age of 3 months. He had recurrent pulmonary infections. He was diagnosed with a patent ductus arteriosus (PDA) and mitral valve prolapse (MVP) at the age of 18 months. He had a coil embolization procedure at the age of 22 months. Head control was present at the age of 15 months, he sat with support at 18 months and walked after the age of 4 years. He had gastroesophageal reflux and had surgery for unilateral cryptorchidism. The sweat chloride test, abdominorenal ultrasonography, sleep EEG, audiological assessment, MRI of the brain and metabolic diagnostics were normal. He had right retinal atrophy and did not have any seizures. His assessment was at the age of 1 $^{10}/_{12}$ years when his height was 71 cm (−4.46 SD), his weight 7 kg (−5.62 SD, BMI: 13.9 kg/m^2) and his OFC 42 cm (−4.6 SD). He could speak two words. Facial dysmorphisms included coarse face, hypertelorism, a broad nasal root and bulbous nasal tip, a full lower vermillion, long philtrum, upslanted palpebral fissures, long eyelashes, bilateral fifth finger clinodactyly and fifth fingernail hypoplasia, as well as hypertrichosis. Unfortunately we did not

get permission to publish his photographs. This boy died from sepsis at the age of 3 years. He had the initial clinical diagnosis of CSS. WES revealed a heterozygous de novo missense mutation in the *KMT2A* gene [NM_001197104.1; chr11:g.118,348,811G>A; c.3464G>A; p.(Cys1155Tyr)], which was rated 'probably damaging' in PolyPhen-2 and is linked to Wiedemann–Steiner syndrome (OMIM #605130). This mutation likely represents the causative variant.

Individual K2571 is the third child of healthy, non-consanguineous parents with an uneventful family history. His mother had three early miscarriages. In the 20th week of gestation hypoplastic left heart syndrome, agenesis of the left kidney and pelvic kidney on the right side were diagnosed. The boy was born spontaneously at 38 weeks of gestation with a birth weight of 2870 g (−1.2 SD), length of 50 cm (+0.1 SD), and OFC of 32 cm (−1.8 SD). APGAR scores were 6/7/8. After delivery prostaglandin infusion was initiated. Hypocalcemia required substitution. After X-ray and ultrasound investigations, the diagnosis of left kidney agenesis could be confirmed. Additionally, diaphragmatic hernia of the right side with herniation of liver into the thorax, a butterfly vertebra Th10 and cervical rib C7 were diagnosed. Ophthalmologic examination was suspicious of sclerocornea. On clinical examination at 3 days, the child was intubated. Facial dysmorphism included upslanting right palpebral fissure, low set and posteriorly rotated ears with asymmetric dysplastic pinnae, a broad nasal bridge and slightly upturned nares, a long flat philtrum with thin upper and full lower vermillion, and a small receding chin (Fig. 2a, b). Shortening of the fifth fingers was noted. All fingernails were dysplastic (Fig. 2c), the fifth fingernails were missing and the fifth toenails seemed hypoplastic (Fig. 2d). Fetal pads of the first toes were noted. Pectus excavatum was present. The boy died at the age of 9 days due to cardio-respiratory insufficiency. He had the initial clinical diagnosis of CSS. WES revealed a heterozygous, de novo 1-bp deletion in the *KMT2D* gene [NM_003482.3; chr12:g.49,436,038delG; c.5943delC, p.(Ser1928Pro*fs**65)] which has been linked to Kabuki syndrome (OMIM #147920). This mutation likely represents the causative variant.

This girl (K2576) is the first child of healthy, non-consanguineous parents with an uneventful family history. During pregnancy, a uterus hematoma was diagnosed. She was born at 32 weeks of gestation with a weight of 1110 g (−1.74 SD), a length of 37 cm (−1.7 SD) and an OFC of 27 cm (−1.47 SD). After birth, she was diagnosed with a VSD, an umbilical hernia and showed hypoplasia of the left toes. Retinopathia prematurorum was treated with laser therapy. Aplasia cutis congenita was not mentioned in any letters. Her first assessment was at the age of 7 months when her length was 58 cm (−3.52 SD for corrected age), her weight was 5 kg (−3.7 SD, BMI: 14.86 kg/m^2 for corrected age) and her OFC was 38.5 cm (−3.5 SD for corrected age). She showed narrow palpebral fissures, long eyelashes, a flat nasal bridge and broad nose, a small mouth with a highly arched palate, localized hair thinning, and three small scars on her scalp which was indicative of aplasia cutis congenita (Fig. 2e, f, i). Her fifth fingernails as well as the fourth and fifth right toenails were hypoplastic (Fig. 2g). The left foot showed short phalanges, a cutaneous II–IV syndactyly, absent second, third and fifth toenails and hypoplastic first and fourth toenails (Fig. 2h). She still showed the umbilical hernia and a rectus diastasis. Her second assessment was at the age of 1 $^{8}/_{12}$ years, her length was 74 cm (−2.94 SD), her weight 8 kg (−3.85 SD, BMI: 14.61 kg/m^2) and her OFC 44.5 cm (−2.64 SD). She sat at the age of 12 months, walked independently at 18 months and said first words at 15 months. MRI of the brain displayed delayed myelination. The VSD had spontaneously closed. Her initial clinical diagnosis was CSS. WES did not identify any de novo variants, therefore, we analyzed for homozygous and compound heterozygous variants. This analysis revealed compound heterozygosity for two inherited variants in the *DOCK6* gene [NM_020812.3; chr19:g.11,332,640T>C; c.3437A>G; p.(His1146Arg); paternal] and [NM_020812.3; chr19:g.11,313,160C>A; c.5362-1G>T maternal]. The first variant was rated 'probably damaging' in PolyPhen-2. The second variant affects the invariant splice-acceptor of intron 42, and aberrant splicing is most probable. In combination with her clinical phenotype including aplasia cutis congenita and mildly malformed limbs, we established the likely diagnosis of Adams–Oliver syndrome (OMIM #614219).

This boy (K2468) is the second child of healthy, non-consanguineous parents with an uneventful family history. Pregnancy was induced by intracytoplasmatic sperm injection. The patient was born at 38 weeks of gestation with a weight of 3270 g (−0.1 SD), a length of 55 cm (+1.7 SD) and OFC of 35 cm (+0.07 SD). He was diagnosed with atrial and ventricular septal defects (ASD and VSD) and underwent surgery at the age of 10 months. He sat at the age of 18 months, walked at 24 months and spoke first words at about 30 months. MRI of the brain and metabolic diagnostics were normal. The sleep EEG was abnormal (possible sharp waves), but he showed no seizures. His first assessment was at the age of 3 $^{9}/_{12}$ years when his height was 108 cm (+1.58 SD), his weight was 21 kg (+2.05 SD, BMI: 18 kg/m^2) and his OFC was 52 cm (+0.72 SD). He could speak two words. Facial dysmorphisms included hypertelorism, epicanthal folds, a wide nasal bridge, hypoplastic alae nasi, a full lower vermillion as well as small and protruding ears (Fig. 2j–m). His second assessment was at the age of 7 $^{4}/_{12}$ years, his height was 131 cm (+1.23

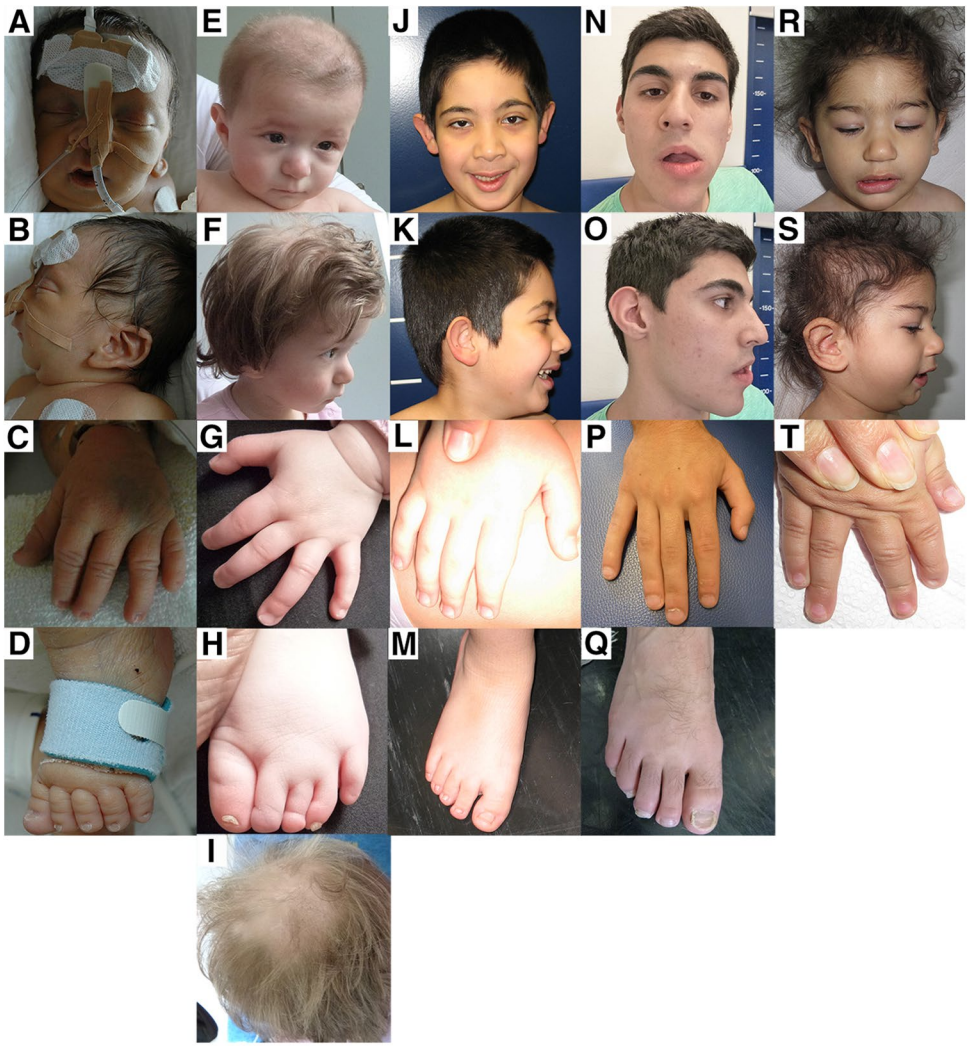

Fig. 2 Clinical photographs of patients with differential diagnoses to BAFopathies. **a–d** K2571 (*KMT2D* 1-bp deletion, Kabuki syndrome), shortly after birth. He presents with proptosis, low-set and mildly dysplastic ears, aplasia of fifth finger- and hypoplasia of fifth toenails. **e–i** K2576 (compound heterozygous *DOCK6* variants, Adams–Oliver syndrome) has localized hair thinning, aplasia cutis congenita, brachytelephalangy of fingers and transverse defect of the left foot with absence of nails II and III and hypoplasia of nails I, IV and V. (**e** 7 months, **f–i** 1 $^{8}/_{12}$ years) **j–m** K2468 (*GRIN2A* frameshift variant) at the age of 3 $^{9}/_{12}$ years has coarse facial features, thick eyebrows, an everted lower lip and hypoplastic distal phalanges. **n–q** K2512 (*SHANK3* splice site variant) presents with mild facial dysmorphisms consisting of coarseness, thick eyebrows and full lower lip at the age of 18 years. He has brachytelephalangy of both hands and feet and hypoplasia of fifth toenail. **r–t** K2446 (so far unsolved) aged 1 $^{5}/_{12}$ years has sparse hair, coarse facial features, full lower lip and hypoplastic fingernails, especially fingers II and V

SD), his weight 38 kg (+2.31 SD, BMI: 22.1 kg/m^2) and his OFC 54 cm (+1.43 SD). He presented with severe ID, was extremely restless and did not keep eye contact. The parents reported that he wakes up between 4 am and 5 am every morning and is very aggressive. In the meantime, he had shown seizures and was treated with Sultiame. Facial dysmorphisms included hypertelorism with long palpebral fissures, midface hypoplasia and a full vermillion of the lower and thin vermillion of the upper lip. His face appeared coarser than in the previous assessment. His hands were short and broad with brachytelephalangy and he had broad feet with fifth nail hypoplasia. Some features were reminiscent of the CSS/NCBRS spectrum. WES revealed a previously undescribed heterozygous de novo deletion in the *GRIN2A* gene [NM_001134407.2; chr16:g.8,857,208_9,857,212delTCATT; c.4189_4193delAATGA; p.(Asn1397Gln*fs**23)]. The individual K2468 shows the typical characteristics of patients with mutations or disruptions of the *GRIN2A* gene such as epilepsy, ID and behavioral problems. Thus, the 5-bp deletion within the *GRIN2A* gene likely represents the causative variant.

Individual K2512 is the second child of healthy, non-consanguineous parents with an uneventful family history. He has an unaffected brother. The patient was born at 40 weeks of gestation with a weight of 3810 g (+0.42 SD), a length of 55 cm (+1.10 SD) and OFC of 36 cm (+0.3 SD). He sat at the age of 8 months, walked at 14 months and did not show any speech development. He was diagnosed with autism before the age of 4 years. MRI of the brain was normal. The EEG was abnormal (spike waves and sharp waves), he showed first seizures at the age of 12 $^{3}/_{12}$ years and was treated with Sultiame. His first assessment was at the age of 13 $^{10}/_{12}$ years when his height was 147 cm (−1.93 SD), his weight was 33 kg (−2.52 SD, BMI: 15.27 kg/m^2) and his OFC was 52 cm (−1.71 SD), his second assessment was at the age of 18 years. He had

a hoarse voice and could not speak any words, he spoke repetitive syllables. He showed body hirsutism, a low frontal hairline, synophrys, thick eyebrows, long eyelashes, a short philtrum, a large mouth with a thick vermillion of the lower lip and macroglossia (Fig. 2n–q). His hands had short distal phalanges. He did not keep eye contact and was very restless. Some features were suggestive of the CSS/NCBRS spectrum, such as the hypoplastic fifth toenails. WES revealed a previously undescribed heterozygous de novo mutation in intron 19 of the autism spectrum disorder gene *SHANK3* [NM_033517.1; chr22:g.51,153,376G>A; c.2265 + 1G>A], which is likely to cause skipping of exon 19, frame-shift and premature stop of translation.

Individual K2446 is the first child of healthy, non-consanguineous parents with an uneventful family history. The girl was born at 40 weeks of gestation via caesarian section with a weight of 3500 g (+0.06 SD). Birth length and head circumference were not assessed. She received phototherapy for indirect hyperbilirubinemia. She had an episode of urinary tract infection at 2 months of age. Denver developmental screening test revealed delays in fine and gross motor developmental milestones. She sat without support at the age of 3.5 years and she still could not walk at the age of 4 years. She spoke first words after 15 months. She did not have any seizures. MRI of the brain at 1 year of age, conventional karyotyping in blood lymphocytes and metabolic tests were normal. Her first assessment was at the age of 17 months. Her height was 74.5 cm (−1.65 SD), her weight 7700 g (−3.57 SD, BMI: 13.9 kg/m^2) and her OFC was 42 cm (−3.35 SD). She could speak two words. Facial dysmorphisms included hypertelorism, epicanthal folds, a broad nasal root, bulbous nasal tip, a full lower and thin upper vermillion, and a small and mildly anteverted ears (Fig. 2r, s). She had long eyelashes, thick eyebrows, sparse hair and hypoplastic second fingernail (Fig. 2t). Her second assessment was at the age of 2 $^2/_{12}$ years. Her height was 82 cm (−1.43 SD), her weight 8850 g (−3.66, BMI: 13.1 kg/m^2) and her OFC 42 cm (−3.84 SD). She spoke 3–4 words, she could not sit without support. Her ophthalmic examination and audiological assessment were normal. The parents reported that she was restless with foreign people. Her face appeared coarser than in the previous assessment. Her hands were short and broad with brachytelephalangy and she had deep palmar creases. Her last assessment was at the age of 4 years. Her height was 93 cm (−1.9 SD), weight was 11 kg (−3.48 SD, BMI: 12.7 kg/m^2) and head circumference was 43 cm (−4.95 SD). She could not walk and speak in sentences. She was attending a special education center. She has the tentative clinical diagnosis of CSS. WES revealed no de novo, homozygous or likely compound heterozygous pathogenic variants in known or potential disease-associated genes.

Discussion

Advantages of WES as a diagnostic tool

In this study, we performed WES in ten individuals with the tentative diagnosis of CSS/NCBRS, and identified causative mutations in nine individuals. Our inclusion criteria for this study comprised ID/developmental delay in individuals older than 6 months and at least one of the following features: hypoplastic fifth nails, coarseness of the face, sparse hair. Surprisingly, four individuals displayed variants in known CSS/NCBRS genes, which were previously analyzed but missed in the Haloplex target enrichment followed by next-generation sequencing and bioinformatic analysis. Upon reinvestigation of this data, we found that the large 26 kb *SMARCA4* intragenic deletion of exons 30–35 in individual K2430 was not annotated by the previously used bioinformatics pipeline (Wieczorek et al. 2013), as it was also the case for the de novo 6-bp deletion within the *SMARCA2* gene (c.3457_3462delGATCTG) in individual K2690. Analysis tools can now be added to the pipeline to identify CNVs using Haloplex enrichment. The two causative variants c.2642G>A (K2510) and c.3655G>C (K2589) in the *SMARCA2* gene were correctly called and annotated but missed during the evaluation of this large data set, e.g., the 2642G>A mutation was annotated with a rs number (rs281875185) and therefore was misleadingly filtered out. It is important to note that this previous gene-panel analysis was performed on single cases and not in a trio-based manner, which likely would have detected the two missense mutations.

Our results show the importance of trio-based WES as a diagnostic tool. First, especially in patients with a less distinct phenotype the detection rate of causative mutations is higher in WES than in panel approaches, such as the Haloplex target enrichment for known and candidate CSS/NCBRS genes. In this study, causative mutations in five of the nine patients would have not been discovered with the panel approach so that we conclude that the trio-based WES approach is superior to syndrome-specific panel approaches. This does not include larger panel approaches, such as an ID panel including all known ID genes. General advantages and disadvantages of WES, such as costs and incidental findings, have been discussed elsewhere (de Ligt et al. 2012). Second, the identification of smaller deletions, such as the 26 kb deletion within the *SMARCA4* gene, does not rely on the presence and density of markers as it does in the array-CGH, but on the density of used capture probes. This deletion was not visible in the Affymetrix 6.0 SNP array performed in this individual because the region is represented on the array by only six SNP probes. We conclude that WES is superior to syndrome-specific panel approaches, but acknowledge that costs of WES, incidental

findings and the availability of parental DNA are important factors to keep in mind when choosing between WES and large ID panel approaches.

Variants in components of the BAF complex broaden the clinical CSS/NCBRS spectrum

CSS/NCBRS can be caused by mutations in different BAF complex genes such as *ARID1A*, *ARID1B*, *SMARCA2*, *SMARCA4*, *SMARCB1* and *SMARCE1* (Santen et al. 2012; Tsurusaki et al. 2012; Van Houdt et al. 2012). *SMARCA4* variants account for 11 % of patients with CSS (Kosho and Okamoto 2014). So far, twelve individuals with CSS with *SMARCA4* variants have been described. Ten have missense mutations, and two have small in-frame deletions (p.Lys458_Glu465del and p.Lys546del), concentrated in the ATPase domain and around the helicase/SANT-associated domain, respectively (Kosho and Okamoto 2014; Tsurusaki et al. 2012). Here, we add the thirteenth individual (K2430) and describe the first larger in-frame deletion of 279 codons (aa 1391-1669) of *SMARCA4* in an individual with CSS, which most probably leads to the formation of a truncated protein.

Interestingly, the individual K2430 shows mild facial CSS features with a flat nasal bridge, a broad nose with an upturned nasal tip, a thin upper and thick lower lip vermillion. However, she displays fifth finger- and toenail hypoplasia, which led to the clinical diagnosis. Due to different ethnic backgrounds, a phenotypic comparison to the other individuals with *SMARCA4* variants is difficult but she has one of the mildest facial CSS phenotypes within the *SMARCA4* cohort so far and thus broadens the CSS spectrum.

The three individuals K2510, K2589 and K2690, in whom we identified *SMARCA2* variants display the wide variability of the NCBRS phenotype and genotype (Fig. 1a–l). Thus far, 61 *SMARCA2* mutations have been described in NCBRS individuals, most of which are missense ($n = 59$) and two of which are in-frame deletions and interestingly, all of which are predicted to affect the ATPase *SMARCA2* domain (Sousa and Hennekam 2014). We add three novel mutations to this list. The individual K2510 has the mutation p.(Gly881Glu) within the ATPase domain, at this position other missense mutations have been described before [p.(Gly881Arg), p.(Gly881Val)] (Sousa and Hennekam 2014). This individual does not present with all the features of the typical NCBRS craniofacial phenotype. He does not show the triangular shape of the face, the long philtrum and the thin vermillion of the upper lip. However, he has a broad philtrum with the cupid-bow shape of the upper vermillion which has been previously noted especially in younger individuals with NCBRS (Sousa and Hennekam 2014) and he presented with seizures, sparse scalp hair and body hirsutism.

The individuals K2589 and K2690 show many of the typical NCBRS features, such as sparse scalp hair, progressive facial coarsening with thick nares, broad philtrum, wide mouth as well as thin upper and thick lower vermillion (Fig. 1e–l). Thus, we would expect typical mutations within the ATPase domain in these individuals. However, we found an in-frame 6-bp deletion (p.Asp1153_Leu1154del) in individual K2690 affecting the *SMARCA2* ATPase domain. This is the first individual with NCBRS with a small in-frame deletion; previously described in-frame deletions spanned larger regions, namely exons 20–26 and exons 20–27 (Sousa and Hennekam 2014). Individual K2589 with a typical facial NCBRS but without seizures carries a variant [c.3655G>C; p.(Ala1219Pro)], which is located near but outside the ATPase domain (UniProt, P51531). The only other boy with a *SMARCA2* variant outside of the ATPase domain had a missense mutation in the Bromo domain and displays an overlapping but distinct clinical phenotype to NCBRS (Sousa and Hennekam 2014).

In summary, we have discovered three novel NCBRS mutations. We present an individual with a typical mutation and only some features of the typical facial phenotype (K2510), we identify the first small in-frame deletion affecting the *SMARCA2* ATPase domain in an individual with typical NCBRS (K2690) and we describe the first NCBRS individual with a typical phenotype and an atypical variant outside of the *SMARCA2* ATPase domain (K2589). These results highlight the broad spectrum of NCBRS and begin to elucidate more variable genotypes and phenotypes than previously appreciated.

The broad clinical spectrum of syndromes caused by variants in epigenetic modifiers

In this study, we purposefully avoided strict and numerous inclusion criteria to detect differential diagnoses of CSS/NCBRS and to investigate the milder end of the CSS/NCBRS spectrum as it has been previously shown in individuals with *ARID1B* variants and intellectual disability (Hoyer et al. 2012). Interestingly, we identified variants in two other epigenetic modifiers in the individuals K2431 and K2571. In the boy K2431 we identified a *KMT2A* missense mutation, which was characterized as probably damaging by in silico tools, leading to the likely diagnosis of Wiedemann–Steiner syndrome (WSS) (OMIM #605130). WSS is caused by heterozygous truncating mutations in the *KMT2A* (*MLL*) gene and characterized by long eyelashes, thick or arched eyebrows with a lateral flare, downslanting palpebral fissures, a broad nasal bridge, a wide nasal tip and hypertrichosis of the elbow region (Jones et al. 2012). Some of the six described individuals also present with a thin upper and thick lower vermillion. A causative mutation

in the *KMT2A* gene was identified in five of these individuals. Interestingly, two cases with "atypical WSS" caused by de novo missense or splice site variants in the *KMT2A* gene have been described recently (Strom et al. 2014). One of these two individuals did not display hypertrichosis of the elbow region, but showed long eyelashes, thick eyebrows and thick hair. In this study, we identify another *KMT2A* missense variant p.(Cys1155Tyr) in the boy K2431 and add the eighth patient to the list of seven previously published individuals with WSS and a causative variant in the *KMT2A* gene. No information on hairy elbows is available for this individual. Comparison of the clinical features listed by Strom and colleagues (Strom et al. 2014) with individual K2431 reveals considerable clinical overlap to the CSS/NCBRS spectrum, including developmental delay (8/8), thick eyebrows (8/8), long and thick eyelashes (8/8), hypertrichosis (6/8), wide nasal bridge (8/8) and broad nasal tip (8/8), as well as thin upper and thick lower vermillion (5/8). Mild fifth fingernail hypoplasia as detected in our patient has not been described before. Taken together, the previously published atypical cases and our discovery of another atypical WSS patient suggest that WSS has an extremely broad clinical spectrum and that hypertrichosis of the elbow region is an important but not an obligatory feature especially in atypical WSS patients. Thus, WSS is likely to be an underdiagnosed entity and an important differential diagnosis to the CSS/NCBRS spectrum.

In another boy (K2571, Fig. 2a–d), we identified a 1-bp deletion in the *KMT2D* gene, which leads to a frame-shift and premature stop of translation, establishing the diagnosis of Kabuki syndrome. Kabuki syndrome also comprises a wide clinical spectrum, diagnosis in infancy can be difficult (Bogershausen and Wollnik 2013). It is caused by nonsense ($n = 89$), frame-shift ($n = 82$), missense ($n = 38$), splice site ($n = 21$) and in-frame deletions/insertions ($n = 6$) (Bogershausen and Wollnik 2013). Clinical features include developmental delay, short stature, and a very distinctive facial phenotype with long palpebral fissures, eversion of the lower eyelid, thick eyelashes and characteristic arched eyebrows. The most common abnormalities of the hands include brachydactyly and/or clinodactyly, but hypoplastic nails have been described (Dentici et al. 2014). A recent review on congenital heart defects stated that hypoplastic left heart syndrome was diagnosed in 5 of 121 patients with Kabuki syndrome (4.1 %) (Digilio et al. 2010; Yuan 2013) and it was also diagnosed in individual K2571. Some clinical features are shared with CSS/NCBRS as well as WSS, such as intellectual disability, thick eyelashes, and the thin upper and full lower vermillion. The individual K2571 was mechanically ventilated, but his face appeared coarse, he had a flat nasal bridge, broad nose and upturned nasal tip and a large mouth with thin upper and thick lower vermillion. The clinical finding which led to the initial tentative diagnosis of CSS was the hypoplastic fifth fingernail (Fig. 2c). The presented case emphasizes that Kabuki syndrome is an important differential diagnosis in an individual with a hypoplastic left heart syndrome and reminds us that Kabuki syndrome patients can also show hypoplastic nails and phalanges (Dentici et al. 2014; Yuan 2013).

Interestingly, *KMT2A* and *KMT2D* both code for histone methyltransferases, suggesting that pathogenic variants in epigenetic modifiers, such as the BAF complex and histone methyltransferases, show a wide and overlapping clinical spectrum. Based on this cohort, we conclude that—especially at younger ages—Wiedemann–Steiner and Kabuki syndromes are important differential diagnoses to keep in mind.

The mild end of the Adams–Oliver syndrome spectrum

In addition, we identified a compound heterozygosity for mutations in *DOCK6* in a girl (K2576, Fig. 2e–i) presenting with mild ID, sparse hair, mild aplasia cutis congenita, short distal phalanges of hands, short toes on the left foot and varying degrees of hypo- to aplastic nails of fingers and toes, including the fifth finger. Homozygous variants in *DOCK6* are known to cause Adams–Oliver syndrome (OMIM #614219), a rare developmental disorder with aplasia cutis congenita and terminal limb defects. So far, only four homozygous *DOCK6* mutations have been published one of which is a splice-acceptor-site mutation (Shaheen et al. 2011, 2013). To our knowledge, this individual (K2576) is the first published case with the clinical phenotype of Adams–Oliver syndrome and a compound heterozygous mutation. The clinical features of this girl demonstrate the milder end of the Adams–Oliver spectrum, which can show aplasia or marked hypoplasia of fingers and/or toes at the severe end of its spectrum. Hence, Adams–Oliver syndrome is an important differential diagnosis in mildly affected individuals with localized hair thinning and a mild limb phenotype.

SHANK3 and *GRIN2A*: important autism spectrum disorder genes to keep in mind

We did not find pathogenic variants in BAF complex genes in the individuals K2468 and K2512 presenting with mild facial dysmorphisms (Fig. 2j–q). However, our WES results draw the attention to the two autism spectrum and epilepsy genes *SHANK3* and *GRIN2A*, in which individuals with autism spectrum disorders and epilepsy might carry pathogenic variants more frequently than previously appreciated. We identified a previously undescribed *SHANK3* mutation in a boy (K2510) who presented with severe ID, absent speech and autism and mild craniofacial dysmorphism consisting of coarse facial

feature, low anterior hairline and full lower lip (Fig. 2n–q). Therefore, he resembles the neurobehavioral spectrum of *SHANK3* mutations well. The gene *SHANK3* encodes for scaffold proteins at the post-synaptic density of glutamatergic synapses (Leblond et al. 2014). *SHANK3* haploinsufficiency causes Phelan–McDermid syndrome, which is characterized by moderate to severe ID, absent to severely delayed speech, neonatal hypotonia, and variable facial phenotypes (Phelan and McDermid 2012) and in about 80 % of the cases autistic behavior (Soorya et al. 2013). *SHANK3* mutations have been described in autism spectrum disorders (Durand et al. 2007). In a recently published meta-analysis, a cohort of patients was screened for *SHANK* copy number and coding sequence variants determining that pathogenic *SHANK3* variants were present in 0.69 % of patients with autism spectrum disorders and in up to 2.12 % of patients with autism spectrum disorders combined with ID (IQ $\leq$70) (Leblond et al. 2014). These findings stress the importance of *SHANK3* analysis in patients presenting with autism spectrum disorders and ID. There is no report on craniofacial phenotypes in patients with *SHANK3* variants, so that we view the rather mild facial dysmorphisms of individual K2510 as familial variability. Individual K2468, in whom we identified a *GRIN2A* mutation, partly resembles the phenotype of CSS patients with low frontal hairline, coarse facial features, thick lower lip, hirsutism, he showed no fingernail hypoplasia and only mild fifth toenail hypoplasia now stressing the importance of these features in CSS (Fig. 2j–m). As *ARID1B* mutation carriers do present with similar, but unspecific clinical findings (Hoyer et al. 2012), we initially established the tentative diagnosis CSS in him. The gene *GRIN2A* encodes for the NRA2 subunit of the NMDA receptor, which is important for neuronal maturation and excitatory synaptic transmission, and was found to be mutated (or disrupted by translocation) in patients with epilepsy, intellectual disability and behavioral problems (Endele et al. 2010). *GRIN2A* mutations were later reported in 4 out of 44 patients with epilepsy-aphasia spectrum disorder (Carvill et al. 2013). The detected variant in the *GRIN2A* gene likely explains his neurobehavioral phenotype including epilepsy and intellectual disability, whereas it remains unclear whether his facial phenotype is due to familial variability. The identification of *SHANK3* and *GRIN2A* variants in these individuals shows that it is important to also consider unspecific neurobehavioral/ID genes during the evaluation of patients with a tentative syndrome diagnosis.

In summary, our study emphasizes the value of WES as a diagnostic tool and discloses important differential diagnoses to CSS/NCBRS. It extends the clinical spectrum of other syndromes caused by pathogenic variants in epigenetic modifiers, such as Wiedemann–Steiner syndrome and broadens the phenotype and genotype spectrums of CSS and NCBRS.

Acknowledgments We are grateful to the families for participating in this study and we thank Sabine Kaya and Daniela Falkenstein for excellent technical assistance. This work was supported by the German Ministry of Education and Research in the frame of the E-RARE network CRANIRARE-2 to DW (BMBF 01GM1211B) and BW (BMBF 01GM1211A), E-Rare-2 (TARGET-CdLS) by the German Federal Ministry of Education and Research (BMBF) to FJK.

References

Berland S, Alme K, Brendehaug A, Houge G, Hovland R (2011) PHF6 deletions may cause Borjeson–Forssman–Lehmann syndrome in females. Mol Syndromol. 1:294–300. doi:10.1159/000330111

Bogershausen N, Wollnik B (2013) Unmasking Kabuki syndrome. Clin Genet 83:201–211. doi:10.1111/cge.12051

Carvill GL et al (2013) GRIN2A mutations cause epilepsy-aphasia spectrum disorders. Nat Genet 45:1073–1076. doi:10.1038/ng.2727

Coffin GS, Siris E (1970) Mental retardation with absent fifth fingernail and terminal phalanx. Am J Dis Child 119:433–439

Crawford J et al (2006) Mutation screening in Borjeson–Forssman–Lehmann syndrome: identification of a novel de novo PHF6 mutation in a female patient. J Med Genet 43:238–243. doi:10.1136/jmg.2005.033084

de Ligt J et al (2012) Diagnostic exome sequencing in persons with severe intellectual disability. N Engl J Med 367:1921–1929. doi:10.1056/NEJMoa1206524

Dentici ML et al (2014) Kabuki syndrome: clinical and molecular diagnosis in the first year of life. Arch Dis Child. doi:10.1136/archdischild-2013-305858

Digilio MC, Baban A, Marino B, Dallapiccola B (2010) Hypoplastic left heart syndrome in patients with Kabuki syndrome. Pediatr Cardiol 31:1111–1113. doi:10.1007/s00246-010-9773-y

Durand CM et al (2007) Mutations in the gene encoding the synaptic scaffolding protein SHANK3 are associated with autism spectrum disorders. Nat Genet 39:25–27. doi:10.1038/ng1933

Endele S et al (2010) Mutations in GRIN2A and GRIN2B encoding regulatory subunits of NMDA receptors cause variable neurodevelopmental phenotypes. Nat Genet 42:1021–1026. doi:10.1038/ng.677

Hoyer J et al (2012) Haploinsufficiency of ARID1B, a member of the SWI/SNF-a chromatin-remodeling complex, is a frequent cause of intellectual disability. Am J Hum Genet 90:565–572. doi:10.1016/j.ajhg.2012.02.007

Jones WD et al (2012) De novo mutations in MLL cause Wiedemann–Steiner syndrome. Am J Hum Genet 91:358–364. doi:10.1016/j.ajhg.2012.06.008

Kosho T, Okamoto N (2014) Genotype–phenotype correlation of Coffin–Siris syndrome caused by mutations in SMARCB1, SMARCA4, SMARCE1, and ARID1A. Am J Med Genet C Semin Med Genet 166C:262–275. doi:10.1002/ajmg.c.31407

Leblond CS et al (2014) Meta-analysis of SHANK mutations in autism spectrum disorders: a gradient of severity in cognitive impairments. PLoS Genet 10:e1004580. doi:10.1371/journal.pgen.1004580

Lower KM et al (2002) Mutations in PHF6 are associated with Borjeson–Forssman–Lehmann syndrome. Nat Genet 32:661–665. doi:10.1038/ng1040

Malak R, Kotwicka M, Krawczyk-Wasielewska A, Mojs E, Samborski W (2013) Motor skills, cognitive development and balance

functions of children with Down syndrome. Ann Agric Environ Med 20:803–806

Nicolaides P, Baraitser M (1993) An unusual syndrome with mental retardation and sparse hair. Clin Dysmorphol 2:232–236

Phelan K, McDermid HE (2012) The 22q13.3 deletion syndrome (Phelan–McDermid syndrome). Mol Syndromol. 2:186–201 (000334260)

Raggio DJ, Massingale TW, Bass JD (1994) Comparison of Vineland Adaptive Behavior Scales-Survey Form age equivalent and standard score with the Bayley Mental Development Index. Percept Mot Skills 79:203–206. doi:10.2466/pms.1994.79.1.203

Santen GW et al (2012) Mutations in SWI/SNF chromatin remodeling complex gene ARID1B cause Coffin–Siris syndrome. Nat Genet 44:379–380. doi:10.1038/ng.2217

Shaheen R et al (2011) Recessive mutations in DOCK6, encoding the guanidine nucleotide exchange factor DOCK6, lead to abnormal actin cytoskeleton organization and Adams–Oliver syndrome. Am J Hum Genet 89:328–333. doi:10.1016/j.ajhg.2011.07.009

Shaheen R et al (2013) Mutations in EOGT confirm the genetic heterogeneity of autosomal-recessive Adams–Oliver syndrome. Am J Hum Genet 92:598–604. doi:10.1016/j.ajhg.2013.02.012

Soorya L et al (2013) Prospective investigation of autism and genotype–phenotype correlations in 22q13 deletion syndrome and SHANK3 deficiency Mol. Autism 4:18. doi:10.1186/2040-2392-4-18

Sousa SB, Hennekam RC (2014) Phenotype and genotype in Nicolaides–Baraitser syndrome. Am J Med Genet C Semin Med Genet 166C:302–314. doi:10.1002/ajmg.c.31409

Sousa SB et al (2009) Nicolaides–Baraitser syndrome: delineation of the phenotype. Am J Med Genet A 149A:1628–1640. doi:10.1002/ajmg.a.32956

Strom SP et al (2014) De Novo variants in the KMT2A (MLL) gene causing atypical Wiedemann–Steiner syndrome in two unrelated individuals identified by clinical exome sequencing. BMC Med Genet 15:49. doi:10.1186/1471-2350-15-49

Tsurusaki Y et al (2012) Mutations affecting components of the SWI/SNF complex cause Coffin–Siris syndrome. Nat Genet 44:376–378. doi:10.1038/ng.2219

Tsurusaki Y et al (2014) De novo SOX11 mutations cause Coffin–Siris syndrome. Nat Commun 5:4011. doi:10.1038/ncomms5011

Van Houdt JK et al (2012) Heterozygous missense mutations in SMARCA2 cause Nicolaides–Baraitser syndrome. Nat Genet 44(445–449):S441. doi:10.1038/ng.1105

Wieczorek D et al (2013) A comprehensive molecular study on Coffin–Siris and Nicolaides–Baraitser syndromes identifies a broad molecular and clinical spectrum converging on altered chromatin remodeling. Hum Mol Genet 22:5121–5135. doi:10.1093/hmg/ddt366

Wilson BG, Roberts CW (2011) SWI/SNF nucleosome remodellers and cancer. Nat Rev Cancer 11:481–492. doi:10.1038/nrc3068

Yuan SM (2013) Congenital heart defects in Kabuki syndrome. Cardiol J 20:121–124. doi:10.5603/CJ.2013.0023

Zweier C et al (2014) Females with de novo aberrations in PHF6: clinical overlap of Borjeson–Forssman–Lehmann with Coffin–Siris syndrome. Am J Med Genet C Semin Med Genet 166C:290–301. doi:10.1002/ajmg.c.31408